

## Recovery Based Nanowire Field-Effect Transistor Detection of Pathogenic Avian Influenza DNA

This content has been downloaded from IOPscience. Please scroll down to see the full text.

2012 Jpn. J. Appl. Phys. 51 02BL02

(<http://iopscience.iop.org/1347-4065/51/2S/02BL02>)

View [the table of contents for this issue](#), or go to the [journal homepage](#) for more

Download details:

IP Address: 140.113.38.11

This content was downloaded on 28/04/2014 at 21:49

Please note that [terms and conditions apply](#).

## Recovery Based Nanowire Field-Effect Transistor Detection of Pathogenic Avian Influenza DNA

Chih-Heng Lin\*, Chia-Jung Chu<sup>1,2\*</sup>, Kang-Ning Teng, Yi-Jr Su, Chii-Dong Chen<sup>1</sup>, Li-Chu Tsai<sup>2</sup>, and Yuh-Shyong Yang<sup>†</sup>

*Institute of Biological Science and Technology, National Chiao Tung University, Hsinchu 300, Taiwan*

<sup>1</sup>*Institute of Physics, Academia Sinica, Taipei 115, Taiwan*

<sup>2</sup>*Institute of Organic and Polymeric Materials, National Taipei University of Technology, Taipei 106, Taiwan*

Received September 24, 2011; accepted November 8, 2011; published online February 20, 2012

Fast and accurate diagnosis is critical in infectious disease surveillance and management. We proposed a DNA recovery system that can easily be adapted to DNA chip or DNA biosensor for fast identification and confirmation of target DNA. This method was based on the re-hybridization of DNA target with a recovery DNA to free the DNA probe. Functionalized silicon nanowire field-effect transistor (SiNW FET) was demonstrated to monitor such specific DNA–DNA interaction using high pathogenic strain virus hemagglutinin 1 (H1) DNA of avian influenza (AI) as target. Specific electric changes were observed in real-time for AI virus DNA sensing and device recovery when nanowire surface of SiNW FET was modified with complementary captured DNA probe. The recovery based SiNW FET biosensor can be further developed for fast identification and further confirmation of a variety of influenza virus strains and other infectious diseases. © 2012 The Japan Society of Applied Physics

### 1. Introduction

Enhanced surveillance of influenza requires rapid, robust, and inexpensive analytical techniques capable of providing an accurate analysis of influenza virus strains. Viral isolation culture with immune confirmation of viral antigen is referred to as “gold standard” for laboratory diagnosis of virus infections. However, it is not commonly used for outpatient surveillance due to clinical specimens require incubation for a period of time (2–14 days).<sup>1)</sup> Additionally, the shell vial culture technique is a rapid alternative to conventional tube cell culture for 2 to 3 days but it is still time-consuming and labor insensitive.<sup>2)</sup> Recently, reverse transcriptase polymerase chain reaction (RT-PCR) is a useful technique for the rapid detection of typing and subtyping influenza viruses with high sensitivity less than 1 day.<sup>3)</sup> Rapid antigen detection assay is applied for the molecular recognition of influenza virus that routinely served as point-of-care diagnosis within 30 min but is less sensitive than those of viral culture and RT-PCR. The methods for the detection of biomolecules can be classified according to the labeling requirement. All labeling methods suffer from the fact to be time-consuming, cumbersome and expensive. Recently, the use of silicon-based field-effect transistors (FETs) as biosensors have attracted much attention due to their compact dimensions, real-time response, high sensitivity and label-free detection.<sup>3)</sup> In recent years, different types of silicon-based devices such as silicon nanowire field-effect transistor (SiNW FET) have been demonstrated for the detection of a variety of analytes, such as ions, DNA, proteins, viruses.<sup>4–9)</sup>

However, it is important to note that the lower specificity for RT-PCR, when referenced to viral culture, yielding a higher rate of false positives.<sup>10)</sup> Accurate diagnosis is one of the most critical issues in infectious disease surveillance and management for reducing the morbidity and mortality of illness. The major limitation of these common methodologies for identification of infectious agent is possibly occurring false positive results. In this study, we proposed a novel DNA recovery system that can significantly enhance

the accuracy of molecular recognition using influenza DNA as target. The method was based on the re-hybridization of oligonucleotide DNA target with a recovery DNA, which is completely complementary to the target DNA, to free the DNA probe and thus provide a further confirmation to identify the DNA target. Functionalized silicon nanowire field-effect transistor has been demonstrated previously for ultra-high sensitivity and real-time detection of avian influenza (AI) virus DNA.<sup>4)</sup> In this report, we further demonstrated that specific detection, confirmation and recovery of DNA probe of AI virus DNA could be achieved with SiNW FET using hemagglutinin 1 (H1) DNA as the diagnostic target. This proposed method can be easily adapted to DNA chip or DNA biosensor for recovery of DNA probe and confirmation of target DNA. We proposed that the recovery DNA based biosensor should be very useful for confirmation of influenza virus strains and diagnosis of many other diverse genetic diseases.

### 2. Experimental Methods

#### 2.1 Materials

3-Aminopropyltriethoxysilane (APTES), glutaraldehyde (25%) in aqueous solution, tris(hydroxymethyl)aminomethane hydrochloride (Tris–HCl), and sodium cyanoborohydride (NaBH<sub>3</sub>CN) were purchased from Sigma-Aldrich. Potassium phosphate monobasic and dibasic were purchased from J. T. Baker. AI virus HA DNA sequences were designed based on the past researches.<sup>11,12)</sup> All synthetic oligonucleotides were purchased from MDBio as shown in Table I. Sodium phosphate buffer (Na-PB) was prepared in deionized water (DIW) and its pH was adjusted to 7.0. All other solutions were prepared with DIW (resistance of water was 18.2 MΩ cm) from an ultra-pure water system (Millipore).

#### 2.2 Device fabrication

The SiNWs were made using silicon-on-insulator (SOI) wafers, which offer a layer of high quality single-crystal silicon separated from the bulk substrates by a layer of buried oxide. The SOI wafers are presently the basis of state-of-the-art metal–oxide semiconductor field-effect transistors (MOSFETs) in the mainstream semiconductor industry. SOI-based SiNW sensors were reported previously.<sup>13,14)</sup>

\*These two authors contributed equally to this work.

<sup>†</sup>E-mail address: ysyang@mail.nctu.edu.tw

**Table I.** Sequences of synthetic oligonucleotides.

Oligonucleotides	Sequence
5'-aminommodified H1 captured DNA probe	5'-NH <sub>2</sub> -C <sub>6</sub> -CAC ACT CTG TCA ACC TAC-3'
5'-Cy3-modified H1 target DNA	5'-Cy3-CCA TTG TGA CTG TCC TCA AGT AGG TTG ACA GAG TGT G-3'
5'-Cy3-modified H5 target DNA	5'-Cy3-TGA TAA CCA ATG CAG ATT TG-3'
H1 target DNA	5'-CCA TTG TGA CTG TCC TCA AGT AGG TTG ACA GAG TGT G-3'
H1 recovery DNA	5'-CAC ACT CTG TCA ACC TAC TTG AGG ACA GTC ACA ATG G-3'

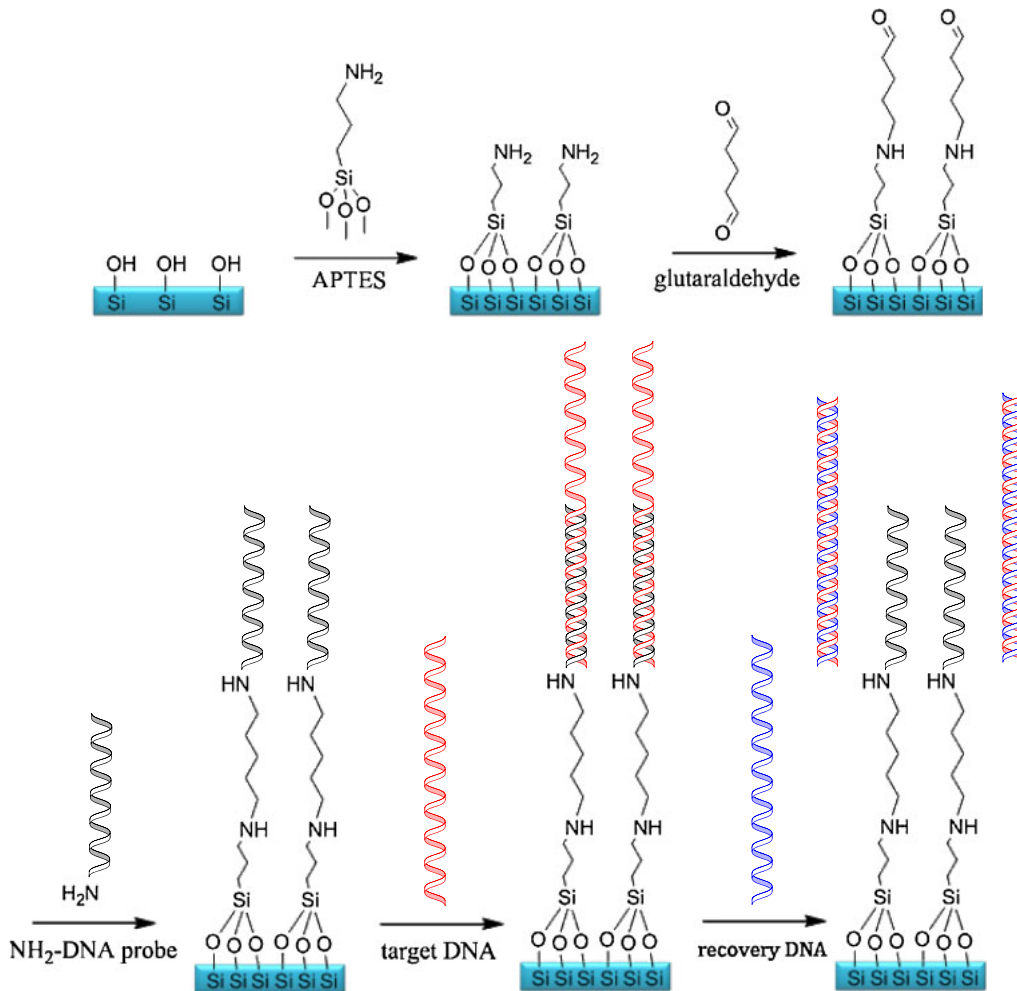


**Fig. 1.** (Color online) Functionalization of SiNW for AI virus DNA detection.

**2.3 Electric measurement of SiNW FET**

The gate potential and source/drain bias voltage were controlled with chip analyzer (Keithley 2636). Generally, in the determination of the  $I_D-V_{DS}$  curve, the drain current ( $I_D$ ) was measured at several constant bias voltage ( $V_{GS}$  from  $-1.0$  to  $-10$  V with a step of  $1.0$  V) while sweeping the  $V_{DS}$  from  $0$  to  $1.0$  V to examine the performance of SiNW FET. In the measurement of the  $I_D-V_{GS}$  curve,  $I_D$  was determined at constant bias voltage ( $V_{DS} = 0.5$  V) while sweeping the gate potential ( $V_{GS}$ ) from  $0$  to  $-15$  V to test the SiNW FET performance in air and aqueous solution. To ensure that the device was in the same initial state, we performed a sweep started at  $-3.5$  V bias. After the stabilized base  $I_D-V_{GS}$  curve was obtained in  $10$  mM Na-PB (pH 7.0), the AI virus target DNA in Na-PB solution was loaded directly into the nano device with microfluidic channel. When comparing  $I_D-V_{GS}$  curve behavior to those of controlled experiments,

we noted that the bio-sensing tests gave the current shift at the same bias conduction. The electric response of DNA/DNA hybridization was observed as soon as the target or recovery DNA was added.

**2.4 Immobilization of H1 DNA probe on the NW surface**

Immobilization of captured DNA probe on SiNW surface was prepared following a four-step procedure as shown in Fig. 1. Prior to immobilizing the DNA molecules, the SiNW FET devices were cleaned for  $5$  min using pure acetone to remove ambient contaminants. The devices were subsequently soaked in ethanol solution containing  $2.0\%$  APTES (Sigma-Aldrich, purity  $99\%$ ) at room temperature for  $1$  h to form a single layer of APTES with amino functional group ( $-NH_2$ ) on the surface. The devices were then cleaned with deionized water and blow-dried with nitrogen to remove the unbound APTES, which was

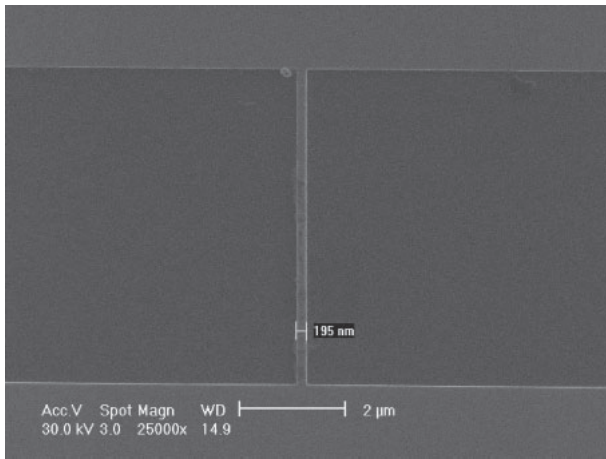


**Fig. 2.** SEM image of SiNW FET device. The width, length and thickness of the wire are 200 nm, 6 μm, and 50 nm, respectively.

followed by bake-drying at 120 °C for 10 min. Secondly, the device surface was covered with solutions of 12.5% glutaraldehyde in 10 mM sodium phosphate buffer (pH 7.0) for 1 h to let one terminal of glutaraldehyde form imide bonds with APTES followed by sodium phosphate buffer (Na-PB) wash. Thirdly, the 1 μM 5'-ammiommodified captured DNA probe was introduced to bind to the APTES-glutaraldehyde on the surface of the nanowire in Na-PB for 4 h. The unbound DNA molecules were then washed away by a large amount of Na-PB solution (10 mM, pH 7.0). Finally, the un-reacted aldehyde groups were blocked by soaking in 10 mM Tris-HCl (pH 7.0) with 4 mM sodium cyanoborohydride for 30 min and the modified device was washed with Na-PB solution.

### 3. Results and Discussion

#### 3.1 Device layout and electric characterization of SiNW FET

The structure of the nano device used in this study was verified using scanning electron microscopy (SEM) as shown in Fig. 2. This is a p-type single crystalline SiNW FET device fabricated based on previously reported methods.<sup>13,14</sup> The wires were defined by standard electron beam lithography and photolithography process and thermally oxidized to form a SiO<sub>2</sub> insulating layer which inhibited charge transferring between attached molecules and wires.<sup>14</sup> The SEM image shows a SiNW channel between the source and drain on the silicon wafer. A significant portion of the SiNW channel (6.0 μm length, 200 nm width, and 50 nm thickness as shown in Fig. 2) was exposed to the environment and served as the sensing site. The source and drain pads were connected to tungsten probe needles to measure the electric properties of the device at room temperature using three probes contact geometries.

The electric properties of the SiNW FET were verified with  $I_D$ - $V_{DS}$ ,  $I_D$ - $V_{GS}$ , and  $I_G$ - $V_{GS}$  curves shown in Fig. 3. The  $I_D$  versus  $V_{DS}$  output characteristics of a representative SiNW FET were shown in Fig. 3(a) for  $V_{GS}$  varying from -1.0 to -10 V with 1.0 V per step. The measured  $I_D$ - $V_{DS}$  characteristics showed that the current of the device between the source and drain was controlled effectively by the potential of the gate electrode. Typical characteristics of

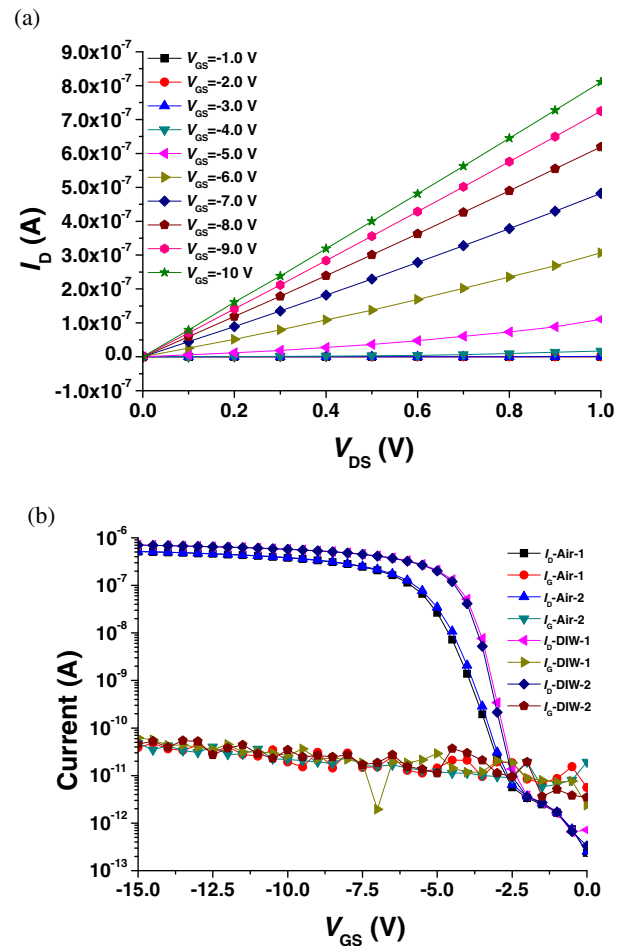


**Fig. 3.** (Color online) Electrical characterization of SiNW FET. (a)  $I_D$ - $V_{DS}$  characteristics of SiNW FET. (b) The  $I_D$ - $V_{GS}$  curves and leakage current of SiNW FET in air and DIW.

SiNW FET at room temperature were shown in Fig. 3(b). The  $I_D$  versus  $V_{GS}$  (from 0 to -15 V) output characteristics with constant  $V_{DS}$  (0.5 V) exhibited excellent semiconductor FET characteristics, illustrating p-type behavior. Good device performance with high on/off current ratio (around 6 orders) and reasonable sub-threshold swing (630 mV/dec) was achieved [Fig. 3(b)]. The  $I_D$ - $V_{GS}$  curve in aqueous solution shown in Fig. 3(b) was similar to that obtained in air. The  $I_D$ - $V_{GS}$  curve remained unchanged in air and in the presence of DIW indicated that the electric property of SiNW FET was stable. Our results indicated that the device can be kept at a low gate leakage current in aqueous condition and this is especially important when highly sensitive transducer is required. SiNW covered with a SiO<sub>2</sub> insulating layer was used to prevent the device from liquid invasion and retain its excellent electrical characteristics and minimal leakage current between back-gate and source/drain electrode in aqueous solution.<sup>14</sup>

#### 3.2 Verification of the DNA recovery system on the surface of silicon base substrate

The proposed DNA target confirmation and probe recovery system is illustrated in Fig. 1. Following the immobilization of the DNA probe on the silicon base substrate, the target DNA hybridized with the probe and could be monitored by a SiNW FET device if the processes were built on the surface

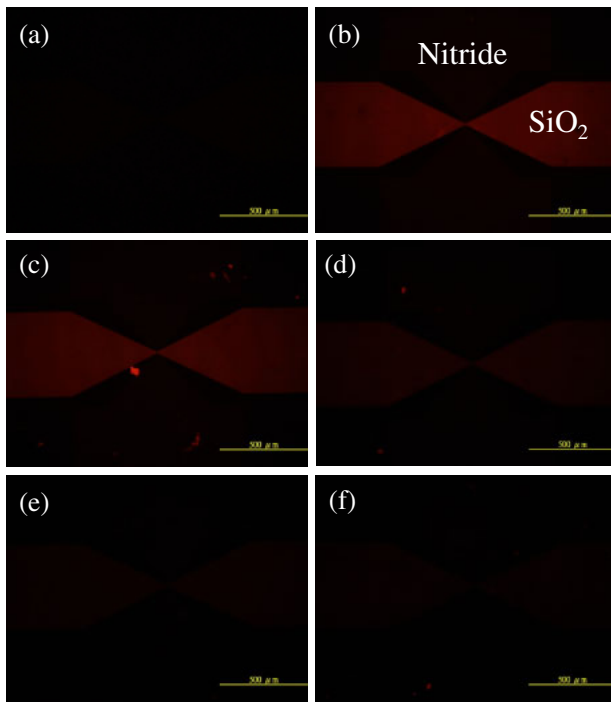


**Fig. 4.** (Color online) Fluorescent microscopic images immobilized H1 captured DNA probe on silicon oxide substrate. (a) Hybridization with non-specific 5'-Cy3-modified H5 target DNA. 5'-Cy3-modified H5 target DNA (100 nM, 1 ml) in 10 mM Na-PB (pH 7.0) was mixed with the immobilized probe following by washing with the buffer three times. (b) Hybridization with specific target DNA. 5'-Cy3-modified H1 target DNA (100 nM, 1 ml) in 10 mM Na-PB (pH 7.0) was mixed with the immobilized probe following by washing with the buffer three times. Removal of 5'-Cy3-modified H1 target DNA with (c) 10 mM Na-PB solution, (d) 100 nM recovery DNA, (e) 500 nM recovery DNA and (f) 1  $\mu$ M recovery DNA in 10 mM Na-PB (pH 7.0, 1 ml) followed by washing with the Na-PB buffer three times. The nitride layer was found to be non-fluorescent throughout the experiments because only the surface of silicon oxide could be modified with APTES as described in Fig. 1.

of the device. The target DNA could re-hybridize with the recovery DNA to free the DNA probe, which could produce another change of electric signal if the event occurred on SiNW FET. With proper design, the reaction will thermodynamically favor the re-hybridization of the target DNA because more complementary nucleotides were available between the target DNA and recovery DNA (Table I). This scheme was first verified through fluorescent labeling of the target DNA as shown in Fig. 4.

The DNA functionalized device could be monitored by fluorescent labeling on H1 target DNA using 5'-cyanine 3 (5'-Cy3) as the fluorescent reporter (Table I and Fig. 4) which produces red light fluorescence under green light excitation. H1 captured DNA probes were first functionalized on the surface of silicon oxide according to the procedure diagramed in Fig. 1. Fluorescence was not observed on the surface of the device following the addition of non-specific 5'-Cy3-modified H5 target DNA under green light excitation [Fig. 4(a)]. This result indicated that non-specific binding of non-complementary target DNA to H1 captured DNA probe functionalized device did not occur. Clear fluorescence was observed in Fig. 4(b) when 5'-Cy3-modified H1 target DNA hybridized with the H1 captured DNA probes immobilized on the silicon oxide surface. As

shown in Fig. 4(b), the nitride layer was found to be non-fluorescent because only the surface of silicon oxide could be modified with APTES and the H1 captured DNA probes. The resulted double helix following hybridization between probe and target DNAs was very stable (18 nucleotide complementary sequence) and could not be easily separated in 10 mM sodium phosphate buffer solution (pH 7.0) as shown in Fig. 4(c). However, the H1 target DNA was clearly removed from the silicon oxide substrate using the H1 recovery DNA (Table I) in the same buffer solution as demonstrated by the disappearance of fluorescence in Figs. 4(d)–4(f). As the results, the fluorescence microscopic images shown in Figs. 4(d)–4(f) revealed that the decreasing fluorescence intensity correlated with the addition of recovery DNA concentration increasing from 100 nM to 1  $\mu$ M. This observation indicated that the disappearance of fluorescence in the microscopic images was specifically affected by the interaction between target and recovery DNA. The recovery DNA contains more nucleotide sequence complementary to H1 target DNA than that of H1 captured probe and is thus thermodynamically more favorable to form a target-recovery DNA duplex. The predicted free-energy change ( $\Delta G$ ) of probe-target DNA duplex and target-recovery DNA duplex in the experimental conditions (10 mM Na-PB at 25  $^{\circ}$ C) were  $-8.94$  and  $-21.2$  kcal/mol, respectively, according to previous study.<sup>15)</sup> This result further confirmed that the target DNA was originally tightly bound to the probe immobilized on the silicon oxide surface and was removed from the DNA probe by the recovery DNA. In addition, this reaction created a free probe that can be used for other experiments. This can be very useful for many studies using DNA as probe for molecular diagnosis as non-specific binding was a general problem.

### 3.3 Electric responses of specific DNA/DNA interactions on SiNW FET

The increase in negative charges resulted from hybridization between target DNA and complementary captured DNA probe can greatly affect the surface conductivity of SiNW FET. For a p-type NW FET, an increase of the current will be expected when negative charges were introduced on its sensing surface. In the SOI-based SiNW sensing devices, several wires were made in the neighborhood on the same chip with similar electrical properties that could be measured simultaneously. This design provides a check for local environment variation.<sup>14)</sup> Figure 5(a) shows  $I_D$ - $V_{GS}$  measurement of the p-type SiNW modified with H1 captured DNA probe. First, Na-PB solution (10 mM, pH 7.0) was added into the microfluidic channel on the functionalized SiNWs as background curve [black square, Fig. 5(a)]. Subsequently, H1 target DNA (100 pM in 10 mM Na-PB, pH 7.0) was introduced to hybridize with the immobilized H1 captured DNA probe on the NW surface, and a clear increase in the drain current of the device was observed [red circle, Fig. 5(a)]. The increased  $I_D$  in the p-type SiNW implies an increased negative charge on the wire surface. This is consistent with the fact that DNA molecules with an isoelectric point of about 5.0<sup>16)</sup> should possess negative charges in a pH 7.0 electrolyte. Subsequently, the H1 recovery DNA (100 nM) in Na-PB solution (10 mM, pH 7.0) was injected into the microfluidic channel to verify

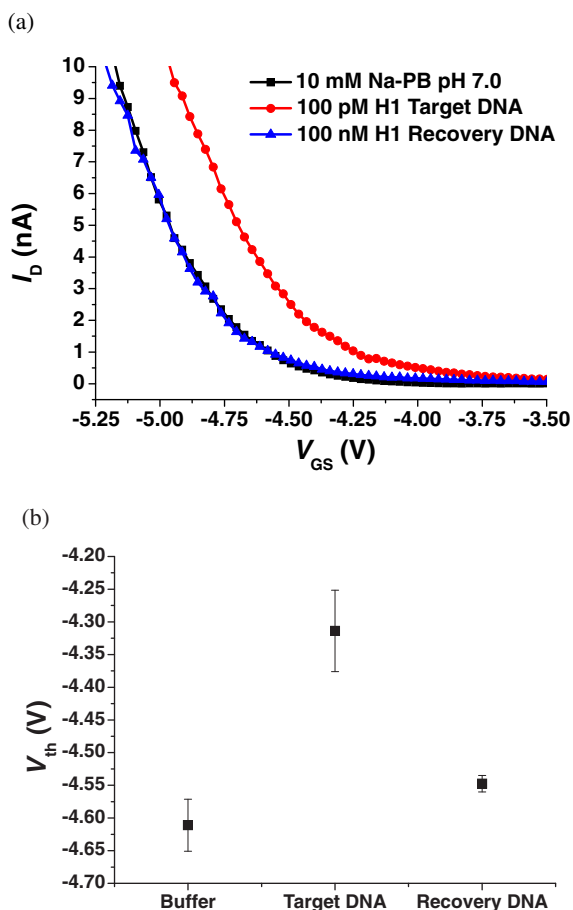


**Fig. 5.** (Color online) Electric responses of functionalized SiNW FET to hybridization and recovery of H1 captured DNA probe. (a)  $I_D$ - $V_{GS}$  curves of functionalized SiNW FET device following hybridization and recovery of H1 captured DNA probe. (b)  $V_{th}$  of H1 captured DNA probe functionalized SiNW FET. The electric properties of SiNW FET were determined under 10 mM Na-PB (pH 7.0), and following by the addition of 100 pM H1 target DNA (200  $\mu$ l) and 100 nM H1 recovery DNA (200  $\mu$ l), respectively. Each data was the average measurements from three devices.

that the electric signal specified to DNA/DNA interaction. The expected change of electric response was observed in the presence of 100 nM recovery DNA [blue triangle, Fig. 5(a)]. The recovery efficiency was nearly 100% according to the current shift following the addition of recovery DNA. Figure 5(b) gives the changes of  $V_{th}$  upon adding 10 mM Na-PB (pH 7.0), 100 pM H1 target DNA and 100 nM H1 recovery DNA, respectively. The  $V_{th}$  shift (0.3 V) in the p-type SiNW implies an increased negative charge from target DNA on the nanowire surface. It was worth to notice that the  $V_{th}$  shift to buffer baseline ( $V_{th} = -4.61$  V) following adding 100 nM recovery DNA ( $V_{th} = -4.55$  V) from three individual devices. The observation provided us important information for future development of recovery based SiNW FET for a variety of biological sensing experiments. The results strongly suggested that specific recovery DNA hybridized with H1 target DNA and thus took it away from H1 capture DNA probe immobilized the SiNW surface. This event induced change of drain current and brought it back to the baseline current of DNA probe only device. This also indicated that a recovery based sensing device for the specific diagnosis of AI virus infection

can be achieved. At present, the profile change in the  $I_D$ - $V_{GS}$  curve gave an extra mean to distinguish the  $V_{th}$  changes caused by non-homogeneity of the device or by the DNA/DNA hybridization. The disparities in  $I$ - $V$  characteristics between devices do not affect the bio-sensing event, which was determined according to the electric changes in each device. This variation can be eliminated or greatly improved in the future when the procedures for the SiNW FET fabrication become standardized. This is the first report for label-free detection of AI virus DNA with recovery based SiNW FET. In contrast to the conventional DNA chips that were operated by oligonucleotides hybridization,<sup>10,11</sup> this system processed simple, reversible, extensive and biocompatible properties for further confirmation of sequence-specific DNA recognition. In the future, recovery based DNA biosensor might have a great potential to develop a highly specific biosensor for the application of gene discovery and disease diagnosis.

#### 4. Conclusions

We have demonstrated for the first time that semiconducting SiNW FET could be developed to a recovery based biosensor for highly specific detection of AI virus DNA. This would be of great scientific and commercial values and may open the door to real-time molecular diagnosis and direct surveillance of infection diseases.

#### Acknowledgements

This research is financially supported by Department of Health (DOH 99-TD-N-111-003) and MOE-ATU Program.

- 1) R. D. Mills, K. J. Cain, and G. L. Woods: *J. Clin. Microbiol.* **27** (1989) 2505.
- 2) S. Matthey, D. Nicholson, S. Ruhs, B. Alden, M. Knock, K. Schultz, and A. Schmuecker: *J. Clin. Microbiol.* **30** (1992) 540.
- 3) M. P. Lu, C. Y. Hsiao, W. T. Lai, and Y. S. Yang: *Nanotechnology* **21** (2010) 425505.
- 4) C. H. Lin, C. H. Hung, C. Y. Hsiao, H. C. Lin, F. H. Ko, and Y. S. Yang: *Biosens. Bioelectron.* **24** (2009) 3019.
- 5) C. Y. Hsiao, C. H. Lin, C. H. Hung, C. J. Su, Y. R. Lo, C. C. Lee, H. C. Lin, F. H. Ko, T. Y. Huang, and Y. S. Yang: *Biosens. Bioelectron.* **24** (2009) 1223.
- 6) C. H. Lin, C. Y. Hsiao, C. H. Hung, Y. R. Lo, C. C. Lee, C. J. Su, H. C. Lin, F. H. Ko, T. Y. Huang, and Y. S. Yang: *Chem. Commun.* (2008) 5749.
- 7) Z. Gao, A. Agarwal, A. D. Trigg, N. Singh, C. Fang, C. H. Tung, Y. Fan, K. D. Buddharaju, and J. Kong: *Anal. Chem.* **79** (2007) 3291.
- 8) F. Patolsky, G. Zheng, O. Hayden, M. Lakadamyali, X. Zhuang, and C. M. Lieber: *Proc. Natl. Acad. Sci. U.S.A.* **101** (2004) 14017.
- 9) Y. Cui, Q. Wei, H. Park, and C. M. Lieber: *Science* **293** (2001) 1289.
- 10) M. Mehlmann, A. B. Bonner, J. V. Williams, D. M. Dankbar, C. L. Moore, R. D. Kuchta, A. B. Podsiad, J. D. Tamerius, E. D. Dawson, and K. L. Rowlen: *J. Clin. Microbiol.* **45** (2007) 1234.
- 11) X. Han, X. Lin, B. Liu, Y. Hou, J. Huang, S. Wu, J. Liu, L. Mei, G. Jia, and Q. Zhu: *J. Virol. Methods* **152** (2008) 117.
- 12) S. Payungporn, S. Chutinimitkul, A. Chaisingh, S. Damrongwantanapokin, C. Buranathai, A. Amonsin, A. Theamboonlers, and Y. Poovorawan: *J. Virol. Methods* **131** (2006) 143.
- 13) Z. Li, Y. Chen, X. Li, T. I. Kamins, K. Nauka, and R. S. Williams: *Nano Lett.* **4** (2004) 245.
- 14) M. C. Lin, C. J. Chu, L. C. Tsai, H. Y. Lin, C. S. Wu, Y. P. Wu, Y. N. Wu, D. B. Shieh, Y. W. Su, and C. D. Chen: *Nano Lett.* **7** (2007) 3656.
- 15) R. Owczarzy, A. V. Tataurov, Y. Wu, J. A. Manthey, K. A. McQuisten, H. G. Almagbrazi, K. F. Pedersen, Y. Lin, J. Garretson, N. O. McEntaggart, C. A. Sailor, R. B. Dawson, and A. S. Peek: *Nucleic Acids Res.* **36** (2008) 163.
- 16) P. Acharya, P. Cheruku, S. Chatterjee, S. Acharya, and J. Chattopadhyaya: *J. Am. Chem. Soc.* **126** (2004) 2862.